CYCLIC PLASTICITY AND MASING BEHAVIOUR IN METALS AND ALLOYS

H. Abdel-Raouf*, T. H. Topper** and A. Plumtree***

INTRODUCTION

The need for analyzing the cyclic inelastic response and/or fatigue damage is encountered in various applications including nuclear power plants, aerospace and aircraft components. Various transient phenomena occurring during the cyclic deformation of metals have been reported [1] together with an explanation of the associated metallurgical changes [2]. It is also important, however, to study the hysteresis loop shape during cyclic deformation in order to relate the cyclic stress to the strain during the loading history of structural components.

The Bauschinger effect is used to describe the change in the yield stress when the deformation is reversed and is attributed to the development of internal back stress which aids the dislocation motion during the process of load reversal. Masing [3] assumed that either branch of the stress-strain hysteresis loop was geometrically similar to the monotonic stress-strain curve with a scale factor of two. This is often referred to as Masing behaviour and has been widely applied to structural metals under cyclic loading conditions. Morrow and Halford [4] showed that the cyclic stress-strain curve described by the locus of the tips of the various stabilized fully reversed hysteresis loops accurately described the hysteresis loop shape (when magnified by a factor of two). Steady state loop shapes for a wide range of structural metals revealed variations in the tensile and compressive yield strengths although the nonlinear portions of the hysteresis curves remain unchanged in shape [5]. In contrast to Masing behaviour, this is regarded as Non Masing behaviour.

The purpose of the present investigation is to study the hysteresis loop shape and to relate the Bauschinger effect to the cyclic deformation characteristics for a range of metals and alloys. In this manner, the possibility of a particular material displaying Masing and Non Masing behaviour can be assessed and subsequently predicted.

MATERIALS AND EXPERIMENTAL

Nine materials were used in this investigation. These materials together with their heat treatment are presented in Table 1. Strain controlled testing was carried out using a electrohydraulic servocontrolled system. The specimens were cycled at different strain ranges to saturation and the corresponding steady state hysteresis stress-strain loops were plotted.

*Assistant Professor, Cairo University, now visiting Lecturer, Department of Mechanical Engineering, University of Waterloo, Ontario, Canada.
**Department of Civil Engineering, University of Waterloo, Waterloo, Ontario, Canada.
***Department of Mechanical Engineering, University of Waterloo, Waterloo, Ontario, Canada.

RESULTS

The steady state stress-strain hysteresis loops for all the materials tested were translated to a common point at the maximum compressive stress, as shown in Figure 1 and 2. The Bauschinger strain (β) was measured for all the metals in the manner suggested by Wooly [6]. Accordingly, the amount of plastic strain in the reverse direction at 75% of the pre-stress in the forward direction was determined. Thus for cyclic work, using a stable loop, β should be measured at a stress level of

$$\left(\frac{\Delta\sigma}{2} + 0.75\,\frac{\Delta\sigma}{2} = 0.875\,\Delta\sigma\right)$$

87.5% of the saturation stress range as shown in Figure 3. This Bauschinger strain was plotted against the plastic strain range ($\Delta\varepsilon_p$) for the nine materials and is given in Figures 4 and 5. In Figure 4 there is a straight line relationship between β and $\Delta\varepsilon_p$. The group of metals obeying this relationship all displayed Masing behaviour. This group included dispersion hardened aluminum alloys such as 2024-T6 and Al-4% Cu in the hard condition (λ = 0.53 μm), also 1018 steel containing about 30% Martensite and AISI 304 stainless steel. In Figure 5, a nonlinear relation between β and $\Delta\varepsilon_p$ is apparent and correspond to the Non Masing behaviour. All ferritic steels such as 1018 hot rolled, A36 and G 40.11 and nonferrous materials such as commercial purity copper and Al-4% copper alloy (of large interparticle spacing λ = 1.37 μm) are typical examples of this group.

DISCUSSION

Masing Materials

Aluminum alloys 2024-T6 and Al-4% Cu (λ = 0.53 μm) displayed cyclic hardening. The second phase platelets in these heat treated alloys were closely spaced, in fact, were less than the self trapping distance of dislocations. Consequently no dislocation cells formed, even at the high strain ranges. Thus the second phase platelets governed the deformation behaviour. Since this required a high density of geometrically necessary dislocations under steady state conditions, a relatively high internal stress resulted. The deformation of such materials is structurally controlled and independent of the matrix properties.

The plastic deformation behaviour of the 1018 steel containing 30% martensite was also controlled by the structure. It is to be expected that the martensite phase acted in a similar manner to the finely spaced second phase platelets in the aluminum alloys. The AISI type 304 stainless steel, however, is a single phase material but has a low stacking fault energy at room temperature. Cross-slip of dislocations is extremely difficult and no dislocation cells can be expected to form at any of the cyclic strain amplitudes imposed. In this case, dislocation pile ups at the grain boundaries account for the high internal stresses.

Non Masing Materials

Such a group of materials may be regarded as plastically homogeneous and the cyclic deformation controlled by the matrix properties. The underlying property is the high stacking fault energy. On cycling at small strain amplitudes these materials show Masing behaviour and their substructure

contains patches of edge dislocation dipoles. Hardening is governed by the friction stress which is related to the density of the dislocation clusters [7].

Masing behaviour takes place up to a critical cyclic strain range after which Non Masing characteristics appear. The critical strain range ($\Delta\varepsilon_T$) was found to be about 0.0036 for all the ferritic pearlitic steels used and was about 0.0045 and 0.0043 for the Al-4% Cu alloy (λ = 1.37 μm) and commercial purity copper respectively.

At higher cyclic strain amplitudes the substructure revealed dislocation cells. The size of which has been found to be inversely proportional to the saturation stress as defined by the peak stress of the cyclic stress-strain loop [8, 9]. Non Masing behaviour is typical of such conditions. More analysis is needed to relate the cyclic deformation characteristics to the dislocation substructure and is presently under investigation by the authors.

CONCLUSIONS

1. Non Masing behaviour appears to be related to the formation of dislocation cells in a wide variety in metals and alloys.

2. Ferritic pearlitic steels displayed Masing behaviour up to a total strain range of 0.0036, whenever above this level they showed Non Masing characteristics.

3. Masing behaviour was found to be associated with the structure in which no cells were able to form. This was brought about by structurally controlled deformation and as occurred in low stacking energy materials. This behaviour also took place in high stacking fault energy materials if cycled below a critical strain range.

ACKNOWLEDGEMENTS

This work was funded by the National Research Council of Canada.

REFERENCES

1. FELTNER, C. E. and LAIRD, C., Acta Met., 15, 1967, 1372.
2. ABDEL-RAOUF, H., PLUMTREE, A. and BENHAM, P. P., Can. Met. Q., 10, 1970, 87.
3. MASING, G., Proceedings 2nd Int. Congress of Appl. Mechanics, Zurich, 1926.
4. HALFORD, G. R. and MORROW, Jo Dean, Proceedings American Society for Testing and Materials, 62, 1962, 695.
5. JHANSALE, H. R. and TOPPER, T. H., "Cyclic Stress-Strain Behaviour - Analysis, Experimentation, and Failure Prediction", ASTM STP 519, Americal Society for Testing and Materials, 1973, 246.
6. WOOLY, R. L., Phil. Mag., 44, 1953, 597.
7. HAM, R. K., Metals and Metallurgy Trans., 55, 1967, 140.
8. ABDEL-RAOUF, H. and PLUMTREE, A., Met. Trans., 1, 1971, 1863.
9. PRATT, J. E., Acta Met., 15, 1967, 319.

Table 1 Materials and Heat Treatment

Material	Heat Treatment
1. Al-4% Cu (λ = 1.37 μm)	Solution Treated at 540° C for 48 hr. Followed by Water Quench and Aged at 400° C for 6 hr.
2. Al-4% Cu (λ = 0.53 μm) (λ = inter particle spacing)	Solution Treated at 540° C for 48 hr. Followed by Water Quench and Aged at 400° C for 25 min.
3. 2024-T6 Aluminum Alloy	Solution Treated at 540° C for 48 hr. Followed by Water Quench and Aged at 190° C for 12 hr.
4. Commercial Purity Alloy	Annealed at 650° C for 1/2 hr.
5. 1018 Steel	Hot Rolled
6. 1018 Steel	Heat Treated at 760° C for 30 min. Followed by Water Quench, 30% Martensite
7. CSA G40.11 Steel	Hot Rolled (C = .22, Mn = 1.09, Si = .04) %
8. A36-70A	Hot Rolled (C = .11, Mn = 1.06, Si = .27) %
9. AISI 304 Stainless Steel	Quenched from 1000° C

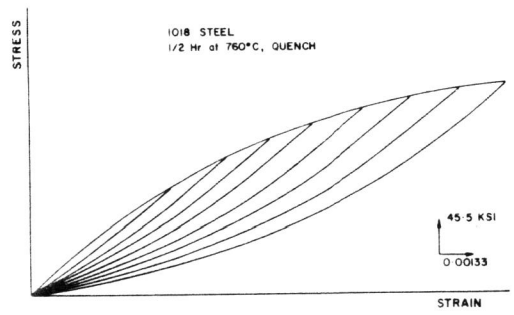

(a) 1018 steel, heat treated, stress 45.5 KSI equivalent to 314 MPa.

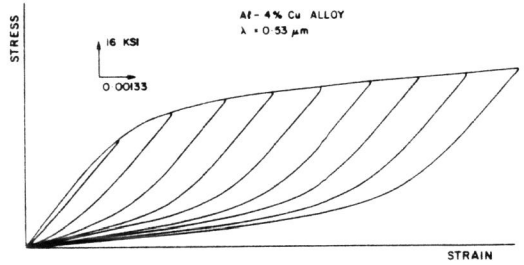

(b) Aℓ-4% Cu (λ = 0.53 μm), stress 16 KSI equivalent to 110 MPa.

Figure 1 Stress-strain hysterisis loops showing masing behaviour.

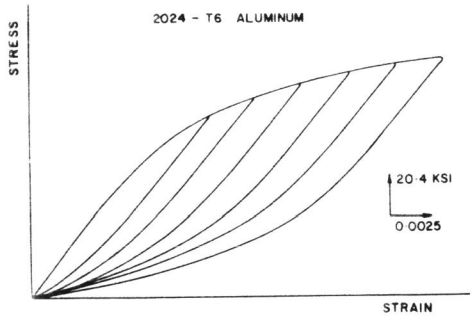

(c) 2024 - T6 Aluminum, stress 20.4 KSI equivalent to 141 MPa.

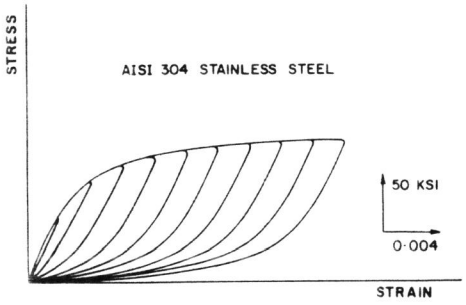

(d) 304 stainless stees, stress 50 KSI equivalent to 345 MPa.

Figure 1

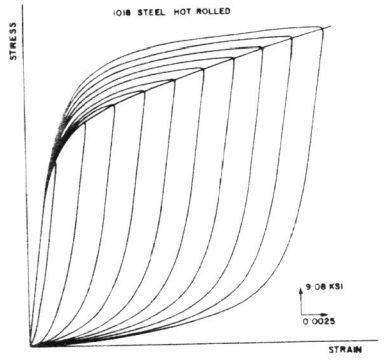

(a) 1018 steel hot rolled, stress 9.08 KSI equivalent to 62.6 MPa.

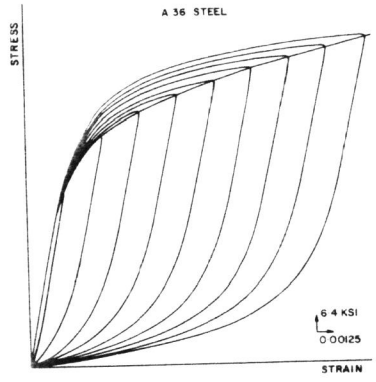

(b) A36 steel, stress 6.4 KSI equivalent to 44 MPa.

Figure 2 Stress-strain hysterisis loops showing non-masing behaviour

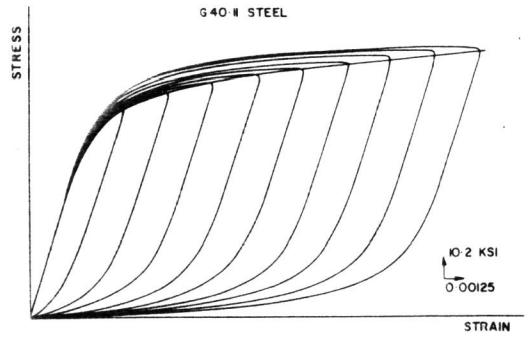

(c) G40.11 steel, stress 10.2 KSI equivalent to to MPa.

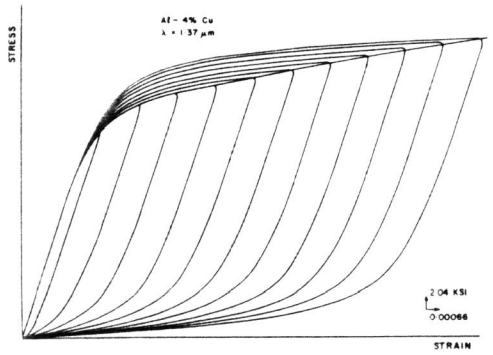

(d) Aℓ - 4% Cu (λ = 1.37 μm) stress 2.04 KSI equivalent to 14 MPa.

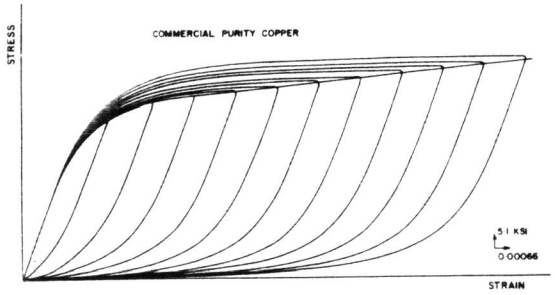

(e) Commercial purity copper, stress 5.1 KSI equivalent to 35 MPa.

Figure 2

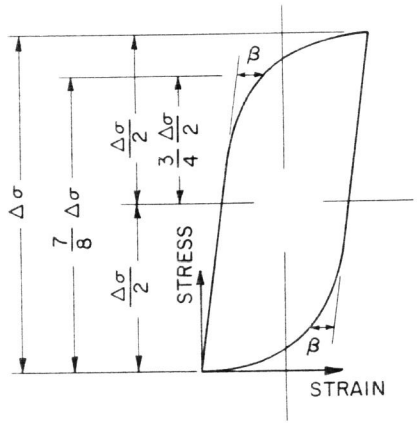

Figure 3 Schematic diagram for the stress-strain loop and β measurements.

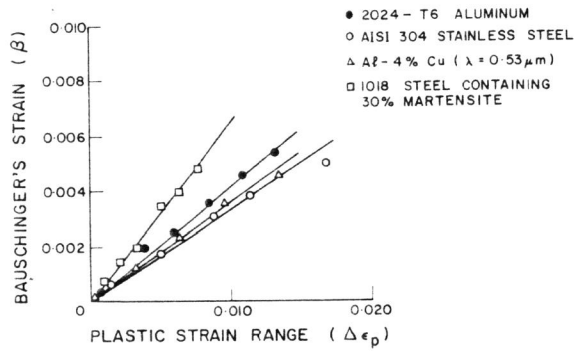

Figure 4 The relationship between Bauschinger strain and plastic strain range for masing materials.

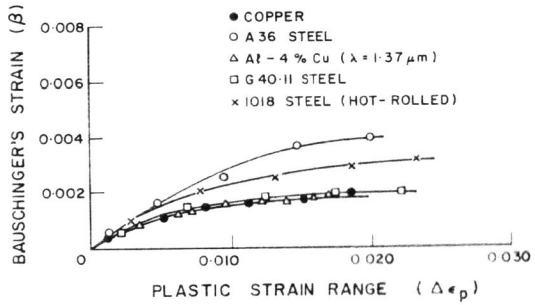

Figure 5 The relationship between Bauschinger strain and plastic strain range for non-masing materials.